REVIEW OF DBER PROGRAM AT LAMPF

October 17-18, 1977

TENTATIVE AGENDA

All meetings in Laboratory Office Building, Room A-234 on the LAMPF site.

Monday, October 17, 1977

8:30 a.m.	Taxi pickup at motel
8:40 a.m.	Taxi pickup at Los Alamos Airport
9:00 - 9:30 a.m.	Committee discussion
9:30 - 10:00 a.m.	"Introduction to LAMPF" L. Rosen
10:00 - 10:45 a.m. Coffee	"Overview of LAMPF Practical Applications and Identification of DBER Programs" J. Bradbury
10:45 - 11:30 a.m.	"Materials Analysis with Muonic X-Rays" R. L. Hutson
11:30 - 12:15	"Proton Computerized Tomography" K. Hanson
12:15 - 1:30 p.m.	Lunch
1:30 - 2:45 p.m.	"Pion Biomedical Program" J. Bradbury, J. Dicello
2:45 - 3:00 p.m.	Coffee
3:00 - 4:00 p.m.	"Biomedical Instrumentation" J.D. Doss
4:00 - 5:00 p.m.	Tour of LAMPF J. Bradbury

Tuesday, October 18, 1977

8:15 a.m.	Taxi pickups as required
8:30 - 11:00 a.m.	Individual discussions
11:00 - 12:00	Executive session

DBER PROGRAM AT LAMPF

Status Report

October 1977

CONTENTS

Section I	Introduction
Section II	Biomedical Instrumentation
Section III	Muonic X-Ray Analysis
Section IV	Proton Computed Tomography
Section V	Pion Biomedical Program
Appendix I	Experiments at Biomed Channel
Appendix II	Selected Reprints

I. INTRODUCTION

The Los Alamos Meson Physics Facility (LAMPF) provides unique high-intensity beams of protons, muons, and pi-mesons. Several of these beams, together with some technological advances realized in developing this facility, are being evaluated for use in the detection and treatment of disease and for application to environmental problems. The DBER program at LAMPF commenced in 1972. This program is conducted by the Practical Applications Group (MP-3) and involves research in three main areas: development and evaluation of biomedical instrumentation, new materials analysis techniques, and the pi meson biomedical program.

The instrumentation development effort (Section II) has been focused mainly on the application of hyperthermia in cancer therapy and new diagnostic possibilities for the detection of cancer. Localized heating techniques have been used on various animal and human tumors. A device for treating the "cancer-eye" condition in cattle has been developed and is now in the commerical sector for marketing. A similar approach may prove useful for some forms of human eye disease. Electronic instrumentation developed at LAMPF for detecting tumors is being tested at several institutions. These techniques are based on indications that tumors differ from normal tissue in temperature and electric potential.

The materials analysis program involves the use of muons (Section III) and protons (Section IV) generated by the LAMPF accelerator. The muonic x-ray spectrum arising from implanting negative muons in a sample has been used to determine the elemental composition of a number of biologically interesting samples. This technique is non-destructive, requires low dose, and can be used to selectively interrogate the interior of bulk specimens. Low-Z elements pose no problem in contrast to most conventional techniques. Experiments have indicated that the x-ray spectrum is also sensitive to the chemical environment in which the muon stops; this should have significance for a number of biological and environmental procedures. Protons are being used to determine the three-dimensional density distribution of objects in a manner analogous to that employed in CAT-scanning with x rays. The advantage of using protons is that a given spatial and density resolution can be achieved with much less dose than with x rays.

The primary objective of the LAMPF pion biomedical program is to evaluate the use of negative pions in cancer therapy. The physical, radiobiological, and

clinical experiments specifically required for this evaluation are performed by LAMPF and University of New Mexico personnel under a grant from the National Cancer Institute. These activities currently require use of the biomedical channel about 60% of operations time. The remaining time is assigned to research of a fundamental nature not designated in the NCI grant and includes pion radiobiology, selected dosimetry and microdosimetry experiments with pion beams, evaluation of new dosimetry techniques, determination of pion W-values and visualization studies. Much of this research is performed by users from institutions other than LAMPF/UNM. The DBER supports the development and operation of the channel for these users and some limited in-house research.

In ensuing sections of this report progress in these areas is described. References are located at the end of each section. Appendices to the report include selected reprints and a list of experiments on the pion biomedical channel.

II. BIOMEDICAL INSTRUMENTATION

A. Background

The design, construction and operation phases of LAMPF have resulted in the creation of a significant technology base, both in terms of personnel and hardware. This resource has been directed toward the solution of several non-accelerator-related problems in the biomedical sphere. The specific technology applied includes radio-frequency techniques, electronic feedback, and monitoring of low-level signals in noisy environments.

B. Localized Tissue Hyperthermia

The results of a number of investigations during the past 25 years show that malignant cells are quite often more sensitive to moderate levels of hyperthermia than their normal counterparts. This information has led to interest in techniques for generating localized thermal fields in tissue for the treatment of cancer, both as the sole modality and in combination with radiation therapy or chemotherapy. Some investigators have reported a synergistic effect from combinations of (low LET) radiation treatments and hyperthermia.

The Practical Applications Group at LAMPF began investigating the utility of localized radio frequency current fields (LCF) for this application during the summer of 1972. (See attached reprint, Med. Instr., 10, Jan-Feb 1976). In this approach, electrodes are placed on (or into) the tissue to create the desired radio frequency current field pattern, with highly localized hyperthermia being the goal. One or more thermistors (mounted in hypodermic needles) are placed into the tissue to be heated; one of these thermistors is used to control the temperature in the tissue via electronic feedback to the rf source. In this manner, temperature (at the control location) can be regulated during therapy to within approximately ± 0.2°C. This hyperthermia method was used in the autumn of 1972 to "treat" transplanted sarcomas on mice obtained from LASL's H-Division. Almost all the tumors regressed after treatments at 45°C for 20 to 30 minutes. In the spring of 1973, a collaboration was arranged with the University of New Mexico Medical School (Dept. of Surgery and Animal Resource Facility) to test the LCF hyperthermia technique in the treatment of spontaneous animal tumors. Arrangements were made with local veterinarians for referral; most of the cases referred were in an advanced state of disease. This work continued through 1974, with the majority of the animals (cats and dogs) experiencing regression of tumor with attendant (apparent) palliation and improvement

of function. A minority of the animals were free of tumor for a follow-up period of 1 to 2 years following treatment. A modified program is continuing at UNM-MS with equipment loans from LASL to test the effectiveness of combined radiation and hyperthermia on similar animal tumors. In the earlier program, LAMPF-designed equipment was also used to test the effectiveness of whole-body hyperthermia in the treatment of advanced canine and feline tumors. This work, while very limited, sparked interest in a whole-body hyperthermia cancer therapy program for humans that is still active at the Albuquerque VA Hospital under direction of the Dept. of Surgery at the UNM Medical School. The localized hyperthermia technique is also being investigated at the UNM Cancer Research and Treatment Center in the experimental treatment of selected human tumors. LAMPF is active with technical input and instruments in this UNM-CRTC clinical effort. LAMPF LCF hyperthermia instrumentation is also currently on loan for use in the very active hyperthermia program at the University of Arizona in Tucson, as well as programs that are just being initiated at the Tufts University Medical School (Boston) and Washington University Medical School (St. Louis).

C. Cancer-Eye Treatment

Results of the LCF animal treatments in 1973-74 raised the question of the applicability of this technique to a disease called "cancer-eye" which has long been almost at epidemic proportions in Hereford cattle. The majority of these tumors are squamous cell carcinoma which occur on the globe or in the lid. A smaller proportion are papillomas or "plaques", both considered to be precursors to the malignant tumor.

Portable LCF treatment equipment was constructed, and arrangements were made through the New Mexico Hereford Association and the USDA Extension Service (NMSU) to test the techniques on two Hereford operations in northern New Mexico. The first animals were treated during June, 1976 and the pilot experiment was complete by March, 1977. Equipment and technique were refined considerably during the ten-month experiment. The final result was a portable LCF treatment unit that could be powered from a vehicle cigarette lighter (or portable battery) and used by ranch workers. When tumors of moderate size are treated (0.2 to 2 cm diameter), approximately 90% remission can be expected with two treatments.

Cancer-eye (or similar) treatment equipment has been loaned to a number of universities and one private research institution for the investigation of

veterinary and human applications. Included in this group are:

University of Arizona (Ext. Service)
New Mexico State University (Ext. Service)
Oklahoma State University (College of Vet. Med.)
McGee Eye Institute, Oklahoma City (Poss. human applications)
University of New Mexico, Cancer Research & Treatment Center
(Now in use in human tumor treatment)
Colorado State University (College of Vet Med.)
(See attached reports: LA-6714-MS and LASL Mini-Review #77-14)

D. Thermal Modification of Corneal Structure

Experimental results reported by Stringer and Parr (Nature, #4965, p. 1307, Dec. 26, 1964) indicated that collagen in the human cornea exhibited a critical shrinkage temperature (58-60°C) that was lower than the shrinkage temperature for collagen in other structures. This information led to the development (at the University of Florida, Gainsville) of a technique called thermokeratoplasty; i.e., the application of heat to the cornea to alter curvature. This technique has involved the application of a preheated metal probe (90 to 130°C) to the cornea for durations of approximately one second. A condition that has been treated with this method is keratoconus, i.e. "cone-shaped cornea". While some clinical success has been reported, there have also been reports of excessive damage to the superficial portion of the cornea, and, in other cases, only transient changes in shape which may be due to insufficient heating of the deeper stromal collagen. Each of these problems may be due to the temperature distribution across the cornea (higher temperatures on the surface) which result from conduction heating.

LAMPF is developing a technique which should reverse the temperature gradient in the cornea so that the important superficial tissue (Bowman's membrane) can be spared while applying sufficient temperature levels to stroma to cause long-term shrinkage. An rf source (2 MHz) with servo control of the rf amplitude applied to the cornea, and precise electronic timing of the duration of the "treatment" has been constructed by LAMPF and loaned to McGee Eye Institute in Oklahoma City for animal tests. Corneal probes have also been loaned, with updated versions being constructed and tested at LAMPF on animal eyes procured from a meat-packing plant in Albuquerque.

The basic technique involves passing rf currents through the cornea with an electrode that is placed into good electrical and thermal contact with the

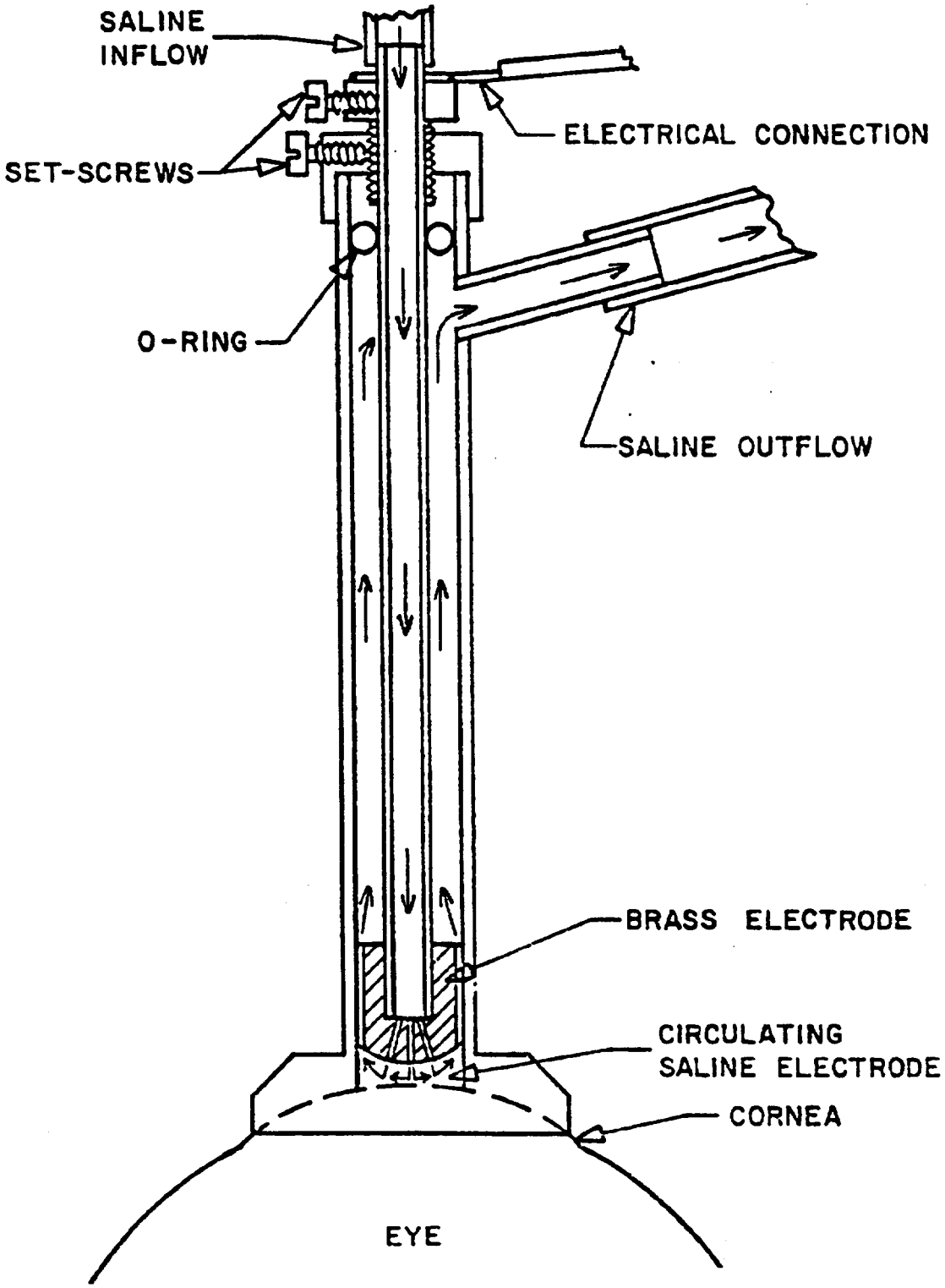

ELECTRODE CONFIGURATION FOR APPLYING HEAT TO CORNEA

tissue. With the appropriate electrode, energy is deposited almost uniformly in the cornea. The electrode is simultaneously cooled to remove heat from the surface of the cornea by conduction. By this combination of deposition of energy by rf current, and cooling of the surface by conduction, it should be possible to achieve a more desirable temperature distribution in the cornea. Initial measurements of the temperature distribution are being made at LASL in dissected animal eyes. Once these data are complete, and probes are considered to be sufficiently well designed, they will be loaned to McGee for further evaluation on living animals. Eventual success of this experiment could lead to treatment of keratoconus (and similar corneal "shape" disorders) without surgery.

E. Bioelectric Potentials in Cancer Diagnosis

There have been reports[1,2] that negative dc electric potentials are usually associated with malignant tumors in laboratory animals and in humans. In one clinical experiment,[3] malignant tumors in the female genital tract were identified by the presence of this electric potential.

LAMPF is collaborating with the University of New Mexico Cancer Research and Treatment Center in a pilot program to investigate the relationship between these potentials and the presence of breast cancer. The first measurements of differential breast-to-breast potential (at UNM-CRTC) were made on September 2, 1977. To date seven subjects have had differential breast potentials recorded. No cases of breast cancer have been measured yet; the seven subjects include "normals" and cases of cancer of the skin, lung and pancreas. Six of the subjects had differential potentials that were typically in the one to five millivolt range. One case, with possible recurrent lung cancer, exhibited a relatively large reading of 18-20 millivolts. Much more data, particularly on proven breast cancer, must be taken in this experiment before even tentative conclusions can be reached.

F. Miscellaneous Projects

The Practical Applications Group has also been involved in the following projects:

1. Design of a portable device for long-term monitoring of differential breast skin temperature for use in breast cancer diagnosis. ERDA was issued a patent on this circuit (#3,960,138 -- 6/1/76). The device is under test at the University of Arizona

Medical School in Tucson. It appears that the device faithfully records the data, but the relevancy of the data for tumor detection has not been definitely established.

2. Two electrosurgical devices have been developed at LAMPF. One of these[4] has been used to cut and seal branch arteries during arterial transplant surgery. The other device is a bi-polar electrosurgical blade, which eliminates the need for the conventional "patient-plate" remote electrode normally used in electrosurgical procedures. The bi-polar blade confines rf current flow to a very small volume of tissue with improved safety and reduced ECG noise. ERDA has applied for a patent (Application Serial No. 601113) on this device.

3. Circuitry has been developed for the removal of electro-surgery-induced noise from ECG monitors.[5]

4. ERDA has been issued a patent (#4,016,886) on the LCF tissue heating technique and is applying for a patent on a load-sensitive oscillator circuit developed for use in the cancer-eye treatment device.

REFERENCES

1. Schauble, M.K., Bullick, H.D., and Habal, M.B., "Variations in tissue electropotentials and their possible significance." Journal of Surgical Research, 12, pp. 325-329 (1972).

2. Schauble, M.K., Habal, M.B. et al, "Electropotentials of tumor tissue." Journal of Surgical Research, 9, pp. 517-520 (1969).

3. Langman, L. and Burr, H.S., "A technique to aid in the detection of malignancy of the female genital tract." American Journal of Obstetrics and Gynecology, 57, pp. 274-281 (1949).

4. Doss, J.D., McCabe, C.W. and Edwards, S., "A New Electrosurgical Coagulating Cutting Forceps," Surgery (Sept. 1973).

5. Doss, J.D., McCabe, C.W. and Weiss, G.K., "Noise-Free ECG Data During Electro-Surgery," Anesthesia and Analgesia..... Current Researches, 52, No. 2, (March-April 1973).

III. MUONIC X-RAY ANALYSIS (MXA)

A. Background

When a negative muon stops in matter it is attracted to an atomic nucleus and cascades down through muonic atom energy levels emitting x rays. The relative yields of muonic x-rays emitted when muons stop in a sample of material provide information about elemental and chemical properties of the material. The total yield within the muonic Lyman series of an element is a measure of the atomic concentration of that element while the relative strengths of the lines within a series are known to be affected by the molecular environment of the element. As part of the experimental program in the LASL Group MP-3 we are measuring muonic x-ray yields from a variety of materials in order to demonstrate the potential usefulness of MXA for major element analysis in problems of biomedical and environmental interest. These experiments also provide fundamental data for testing theoretical models of the muon capture and cascade processes; improved models and predictive capability will increase the applications potential of the technique. The LASL report, LA-5867-MS, included in Appendix II contains a brief discussion of the physical principles involved in the formation of muonic x-rays.

The characteristics of muonic x-ray analysis which may provide advantages over conventional analytical techniques include:

-non-destructive analysis of bulk samples;
-low dose delivered to sample;
-sensitivity to low-Z as well as high-Z elements;
-sensitivity to isotopic and chemical compositions.

We have concentrated our efforts in three areas: 1) development of instrumental configurations and procedures for maximizing count rates and minimizing background, 2) development of data analysis techniques for extracting accurate measures of x-ray yields from the data and 3) examination of a number of samples and evaluation of the results in terms of the potential usefulness of muonic x-ray measurements for materials analysis. A reprint [Radiology 120, 193-198 (1976)] contained in Appendix II discusses items 1) and 2) and the results of a number of sample measurements. Those and more recent measurements are discussed in the next section.

B. Investigations of Tissues and Tissue-like Materials

In the early stages of study of muonic x-rays for sample analysis it was apparent that MXA offered advantages for use in medical diagnosis and biomedical

research. In particular, major-element analysis of tissue volumes as small as a few cubic centimeters located within the body could be performed without giving significant radiation dose to the body and without surgical intervention. We set out to determine if the results of elemental analysis with muonic x-rays matched conventional analysis results closely enough to justify our optimism about the potential of the technique.

The first set of measurements were on animal tissues (muscle, fat, liver, bone, and blood) and on samples of tissue-equivalent plastic and tissue-equivalent liquid. The muonic x-ray measurements of carbon, nitrogen, and oxygen concentrations in the muscle, fat, and liver samples were close to the concentrations obtained with conventional techniques but some unexpected discrepancies were noted. We attributed the differences to errors introduced by the inevitable sampling problem that arose when we tried to get few-gram tissue samples for conventional analysis which were representative of that of the large 100-200 g specimens used in the MXA measurements. The large samples were somewhat inhomogeneous so that the small samples were probably not truly representative. Results from the muonic x-ray studies of the homogeneous materials of well-known composition,e.g. blood, plastic, and tissue-equivalent liquid, gave very close agreement with the known elemental concentrations providing further indication that sampling problems are the source of the discrepancies found with the tissue samples. These results indicate that, for the purpose of analyzing the average composition of relatively large samples, MXA possesses a distinct advantage over those techniques requiring very small samples.

The results of the analysis of the plastic and tissue-equivalent liquid data are given in Table I while Table II [from Radiology 120:193-198 (1976) Appendix II] contains the results of both conventional and muonic x-ray analysis of the various tissue samples.

This work stimulated enquiries from about thirty people from thirteen countries. As a result we were encouraged to continue our studies with tissue with the goal of determining if there are observable differences between normal and pathological tissues. Therefore comparisons were made between the x-ray yields from normal and cirrhotic human liver and between normal dog liver and dog liver tumor.

Two samples each of normal and cirrhotic human liver were studied. For comparison between normal and abnormal samples we calculated the ratios of the

total yields of the oxygen Lyman series x rays to the yields of the carbon Lyman series. These results are shown in Table III where a significant and consistent difference is shown between normal and abnormal tissue. Application of background corrections would tend to increase the difference in the ratios. In addition to the human liver samples we obtained one sample of normal dog liver and one sample of dog liver tumor. The O:C ratio for the normal sample was approximately a factor of two higher than for the tumor sample. It is thus possible that MXA has an application in tumor detection.

Whole-body calcium measurements can be done with neutron activation analysis while bone mineral levels in the arm, for example, can be determined by gamma transmission measurements. However, since localized areas such as the head or spine are somewhat inaccessible with these established techniques, MXA might be useful for analysis in such regions of the body. We obtained two samples of plastic whose calcium and phosphorous concentrations were not identical but approximated those of a typical bone. The ratio of the yield of calcium x rays from one sample to the yield from the other sample and the ratio of phosphorous yields were 1.26 ± 0.10 and 1.61 ± 0.27 respectively, while theory predicts ratios of 1.30 and 1.37. This illustrates that MXA is sensitive to relatively small changes in bone mineral content.

C. Muonic X-Ray Yields from Dilute Solutions

In order to gain a better estimate of the detection limits for relatively low-Z elements, we measured the x-ray yields from dilute solutions of NaF, KCl, $CuSO_4$, and $AgNO_3$. Based on these measurements we conclude that if we do a four-hour irradiation of a thirty-gram sample and use a 10 cc germanium detector we can detect concentrations of 0.1 - 0.5% by weight of elements with Z of about 5, concentrations of 2% for Z of about 20 and concentrations of 5% for Z of 50. Longer irradiations, larger samples, and use of larger detectors would, of course, lead to lower detection limits.

D. Chemical Effects

The above discussion has been directed toward elemental composition studies. In some cases information about the chemical environment of an element in a compound can also be obtained by studying the relative yields of x-ray lines within a series.

1) Hydrogen Effect

It is now well-established that hydrogen in a molecule such as a hydrocarbon alters the x-ray pattern of the carbon Lyman series.[1] Theory doesn't

yet adequately explain this effect. We have begun a series of measurements to

without cutting into the fuel rods. To study this potential application we, in cooperation with other LASL personnel, are going to measure the relative yields of plutonium x rays from their isotopes contained in samples of PuO_2 having different concentrations of the isotopes.

REFERENCES

1. J.D. Knight, C.J. Orth, M.E. Schillaci, R.A. Naumann, H. Daniel, K. Springer, H.B. Knowles, Phys. Rev. A13, No. 1, 43-53 (1976).

TABLE I

RELATIVE MUONIC X RAY YIELDS (%)

	Element	Prediction Based on Known Composition	Measured
Shonka A-150 Plastic	C	87.7 ± 0.4	87.8 ± 0.8
	N	3.7 ± 0.1	3.7 ± 0.2
	O	6.4 ± 0.7	6.5 ± 0.3
	F	1.1 ± 0.1	1.1 ± 0.2
	Ca	1.1 ± 0.1	1.0 ± 0.7
Tissue Equivalent Liquid	C	14.7	14.1 ± 0.6
	N	5.0	3.9 ± 0.2
	O	80.3	81.9 ± 0.6

TABLE II

Table II: Carbon, nitrogen, and oxygen content (per cent by weight) of animal tissue samples

	Sample Description		Carbon Content	Carbon Error	Nitrogen Content	Nitrogen Error	Oxygen Content	Oxygen Error
1.	Pig muscle (1–1),	M	15.45	±0.85	3.47	±0.47	81.08	±0.96
	Liquid nitrogen frozen	C	16.17		3.15		80.68	
2.	Pig muscle (1–1)	M	13.58	0.69	2.80	0.31	83.62	0.75
	Thawed	C	16.17		3.15		80.68	
3.	Pig muscle (1–1),	M	18.05	0.76	3.27	0.27	78.68	0.80
	Refrozen	C	16.17		3.15		80.68	
4.	Pig muscle (1–2),	M	18.07	0.67	3.31	0.28	78.62	0.72
	Liquid nitrogen frozen	C	13.65		3.30		83.05	
5.	Pig muscle (1–3),	M	14.46	1.05	2.93	0.41	82.61	1.12
	Liquid nitrogen frozen	C						
6.	Pig muscle (2–1),	M	10.21	0.85	4.25	0.46	85.29	0.96
	Dry ice frozen	C	16.78		3.36		79.86	
7.	Pig muscle (2–2)	M	14.65	0.89	4.86	0.41	80.49	0.98
	Freezer frozen	C	25.23		3.63		71.14	
8.	Pig muscle (2–3)	M	16.04	0.84	4.48	0.45	79.48	0.95
	Liquid nitrogen frozen	C	12.90		3.55		83.55	
9.	Pig muscle (2–4),	M	15.01	1.02	4.08	0.50	80.91	1.13
	Formalin preserved	C						
10.	Pig fat (1–1),	M	52.96	1.05	1.81	0.21	45.22	1.05
	Liquid nitrogen frozen	C	47.43		2.21		50.37	
11.	Pig liver (1–1),	M	14.81	0.64	3.42	0.29	81.77	0.70
	Liquid nitrogen frozen	C						
12.	Bovine muscle (WA–1),	M	8.56	1.12	4.29	0.59	87.15	1.27
	Liquid nitrogen frozen	C	12.95		3.72		83.32	
13.	Bovine liver (WA–7)	M	13.75	0.70	1.72	0.33	84.52	0.77
	Freezer frozen	C						
14.	Bovine liver (WA–12),	M	12.27	0.74	3.03	0.42	84.70	0.84
	Liquid nitrogen frozen	C	13.36		2.70		83.94	
15.	Dog liver,	M	20.36	0.90	4.07	0.27	75.58	0.94
	Freezer frozen	C						
	Dog blood	M	9.03	0.49	3.14	0.25	87.83	0.55
		C*	10.75		3.23		86.02	
	Bovine bone,	M†	40.68	1.07	3.37	0.20	47.83	1.10
	Freezer frozen	C						

*Human blood composition taken from Reference 15.
†Plus: phosphorus = 1.90 ± 0.29%, calcium = 6.22 ± 0.93%. Normalized so that the sum of all five components is 100%.
C = content as determined by conventional chemical analysis; M = content as determined by muonic x-ray analysis. The data has been normalized so that the sum is 100%. The absolute sums are typically of the order of 85–90%, the remainder being mostly hydrogen.

TABLE III

O:C RATIOS

	NORMAL LIVER		CIRRHOTIC LIVER
#1	1.24 ± .01	#1	1.16 ± .01
#2	1.24 ± .01	#2	1.17 ± .01

IV. PROTON COMPUTED TOMOGRAPHY

A. Introduction

The first phase of this program involved a feasibility study for implementation of a proton computed tomography (CT) system at LAMPF. Calculations were performed to provide a detailed comparison of proton and x ray CT systems. Several reconstruction algorithms were evaluated and applied to simulated proton data. It was determined that protons may be used to produce reconstructed two-dimensional density distributions with accuracy comparable to existing commercial x ray CT units at significantly lower dose levels. The multiple Coulomb scattering which protons undergo as they pass through the specimen is the limiting factor in the spatial resolution.

The experimental implementation of a proton CT scanner at LAMPF constituted the second phase of the program. In this experiment it was shown that the stability required for a competitive proton CT system could be maintained. Proton CT scans were performed on two plastic phantoms designed to test spatial and density resolution. The analysis of the scan data and the subsequent CT reconstructions are presently underway.

B. Density Resolution and Dose Calculations

In the CT method, the two-dimensional density distribution of a specimen is reconstructed from integrated density ($\int \rho dx$) distributions taken through that section at various angles. The proton CT technique consists of obtaining the integrated density distributions, or projections, by measuring the energy lost by protons which traverse the specimen. The uncertainty in the integrated density is determined by the statistical fluctuations which occur in the energy loss process, commonly called straggling. If the energy lost by the proton is experimentally determined by measuring the residual range of the exiting proton in some specified material, the uncertainty in the integrated density is given by the range straggling. Thus, a single 190 MeV proton, which has a range of 23.6 g/cm^2 in water, can provide integrated density to an accuracy of 0.28 g/cm^2.[1]

In order to explore the usefulness of protons in reducing the dose required to obtain a given reconstruction quality, we have computed the dose needed to produce a reconstruction similar to that obtained by the updated EMI head scanner.[2] It was assumed that a 1.3 cm thick slice within a specimen is to be examined with picture elements of dimension 1.5 mm x 1.5 mm. The density resolution desired is 0.4% per picture element.

Use of the Shepp and Logan reconstruction algorithm[3] was assumed in the noise calculation. It was also assumed that the projection measurements are taken from a full 360° range of angles. The proton dose was determined from the ionization energy loss with an RBE = 1. A correction was made for the fraction of incident protons which undergo nuclear interaction rendering them unusable in the energy loss measurement. The x-ray dose was calculated on the basis of the energy absorption coefficient,[3] the back-scatter factor and the depth-dose relation.[4] A monoenergetic x-ray beam was assumed. Figures 1 and 2 show the dependence of the required proton and x-ray dose, respectively, upon the particle energy for 10 cm, 20 cm and 30 cm examination diameters. Table 1 summarizes the doses at the optimum particle energies. It is apparent that protons could provide the same density information as monochromatic x rays with a reduction of the dose by a factor of 3.9 for a 20 cm diameter specimen and a factor of 8.2 for a 30 cm specimen.

C. Spatial Resolution Calculations

A modified Moliére theory of multiple Coulomb scattering was used to determine the spatial spreading of a pencil beam of protons as it passes through tissue. The major portion of the transverse displacement distribution may be approximated by a Gaussian distribution. A Monte Carlo program was used to incorporate proton energy loss. Table II gives the equivalent Gaussian widths for the incident proton energies that would be used to examine 20 and 30 cm thick specimens. A comparison of the resolutions given in Table II with the r.m.s. resolution of present commercial scanners, approximately 1 mm, points to a need to improve the spatial resolution obtainable with protons. One method for obtaining such an improvement is to measure the position of the protons as they exit from the specimen. As depicted in Figure 3, this results in good spatial resolution at entrance and at exit with the worst resolution occurring in the center of the specimen. Another possible approach would be to use heavier charged particles such as alpha particles.[7]

D. Experimental Configuration

In order to demonstrate the feasibility of obtaining high quality CT scans with protons, an experiment was recently performed on the P^3 West channel at LAMPF. The experimental layout is shown schematically in Fig. 4. A specially developed tune of the P^3 channel provided protons in a momentum bite of 0.2%

with a 1.5 mm diameter beam spot. The energy lost by each proton was determined from the measurement of the residual proton energy with a hyperpure germanium (HPGe) detector. The HPGe detector had a diameter of 3.3 cm and a thickness of 1.25 cm. The event trigger was obtained from the two scintillation counters, S1 and S2. S2, with an active diameter of 2 cm, restricted the events to the central region in the HPGe detector. A delay line readout proportional chamber PC, was used to measure the transverse deflection of the proton at the exit of the water bath. During the measurements the phantom was moved across the beam line under computer control. At the end of each traverse, the phantom was rotated by computer command before a new traverse was begun. The use of buffered CAMAC analog-to-digital converters allowed us to acquire data at an average rate of 1000 events per sec with 50% deadtime.

E. Experimental Results

During the early phase of data taking it was demonstrated that the proposed experimental method has sufficient stability to allow us to obtain high quality tomograms. A 210 MeV proton beam was used with a 25.4 cm thick polyethylene degrader in place of the water bath. The residual proton energy was 45 MeV with an r.m.s. width of 4.5 MeV caused by straggling in the polyethylene. Approximately 40,000 events were accumulated in each run to reduce the statistical error in the mean residual energy to 0.023 MeV. In a series of such runs the r.m.s. deviation in the residual energy was found to be 0.041 MeV indicating the presence of systematic uncertainties. These systematic uncertainties are of no consequence when compared with the statistical uncertainties associated with 1,000 events which are needed at each measurement point in an actual tomographic scan. The measured systematic uncertainties imply the r.m.s. drift in the mean momentum of the incident beam is less than 0.004%. The sensitivity of the system was demonstrated by placing a single sheet of Xerox paper in front of the polyethylene. The resulting 0.18 MeV shift of the residual energy, clearly visible in Fig. 5, corresponds to the addition of 0.013 g/cm^2 of polyethylene, or less than 0.06% of the original material thickness.

The data for two CT scans have been taken, and are currently being analyzed. The plastic phantoms had diameters of 20 and 30 cm and were specially designed to facilitate a direct comparison between x-ray and proton scans. Preliminary CT reconstructions have been very encouraging. At dose levels of from 0.5 to 1.0 rads the proton CT reconstructions should have density resolutions

somewhat in excess of those obtainable with present day commercial x-ray scanners which deliver doses up to 10 rads. It is hoped that complete reconstruction will be available in the near future.

REFERENCES

1. R.M. Sternheimer, Phys. Rev. 117, 485-488 (1960).

2. D.P. Boyd, M.T. Korobkin and A. Moss, SPIE 96, Optical Instrumentation in Medicine V, 303-312 (1976).

3. R.D. Evans, Radiation Dosimetry, 2nd E., F.H. Attix and W.C. Roesch, New York, Academic (1968).

4. H.E. Johns and J.R. Cunningham, The Physics of Radiography, 3rd Ed., Springfield, Charles C. Thomas, 1969.

5. V.G. Moliére, Z. Naturforschg. 3a, 78-95 (1948).

6. Physical Aspects of Irradiation, Recommendations of the International Commission on Radiological Units and Measurements, Natl. Bur. Std. (USA) Handbook 85 (1964).

7. T.F. Budinger, et al., Proceedings Image Processing for 2-D and 3-D Reconstruction from Projections, Stanford, CA, August 4-7, 1975.

TABLE I

Comparison of Proton and X-Ray Doses Required to Obtain a 0.4% Density Resolution in 1.5 x 1.5 mm^2 Picture Elements for a 13 mm Thick Section of Water-Like Material

PATH LENGTH, P (G/CM^2)	PROTONS ENERGY (MeV)	PROTONS SURFACE DOSE (RAD)	X-RAYS ENERGY (KeV)	X-RAYS SURFACE DOSE (RAD)	PROTON DOSE ADVANTAGE
10	130	0.010	55	0.026	2.5
20	190	0.032	80	0.12	3.9
30	230	0.065	100	0.53	8.2

TABLE II

Root Mean Square Transverse Displacement of Protons in ICRU Muscle[5] of Unit Density

PROTON ENERGY (MeV)	DEPTH (cm)	R.M.S. RESOLUTION (mm)
190	10	1.2
	20	3.8
230	15	1.9
	30	5.9

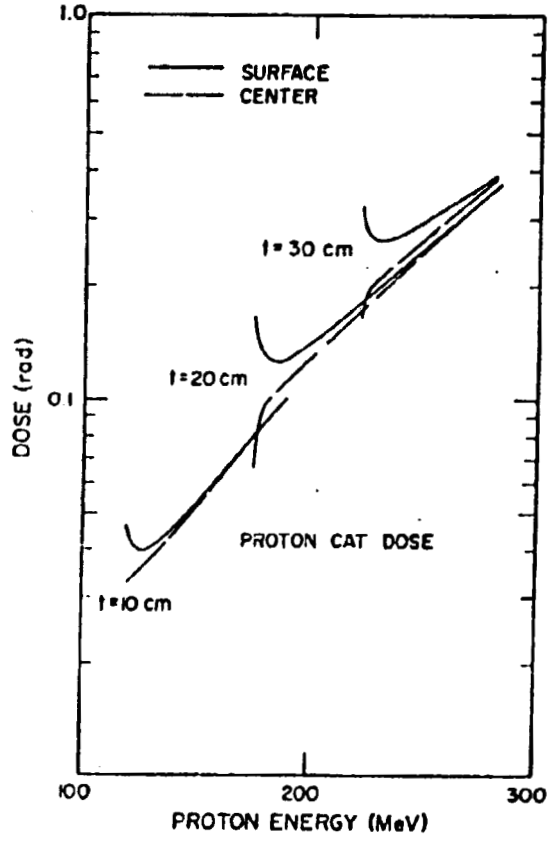

Figure 1

Relative proton dose required to achieve reconstructions of constant density resolution in fixed pixel sizes.

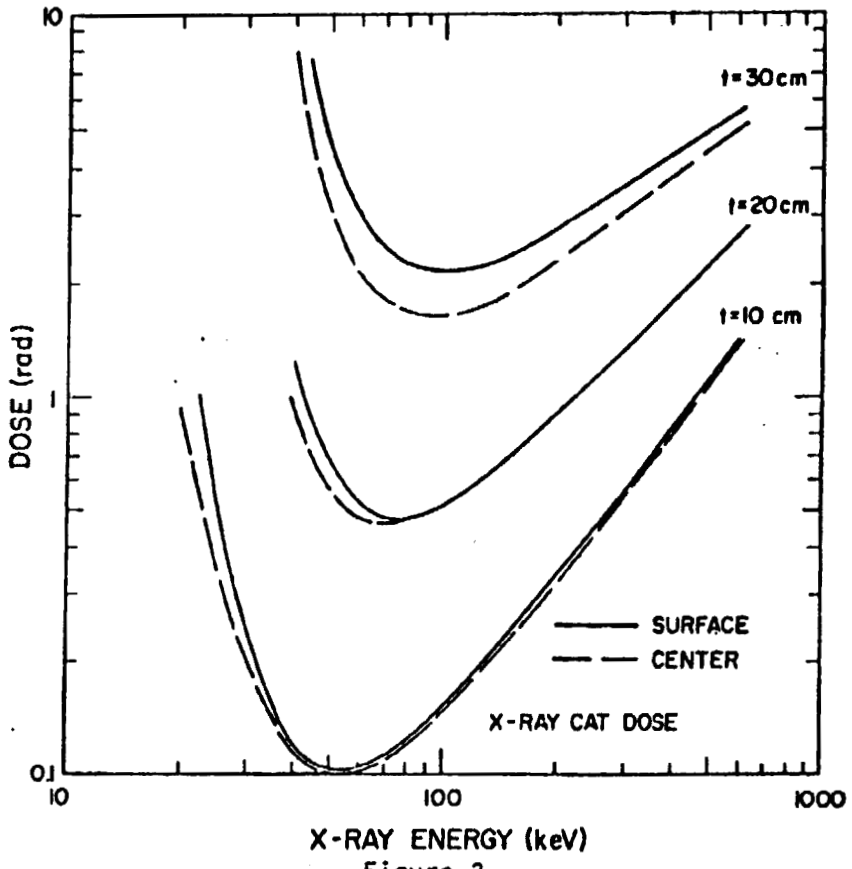

Figure 2

Same as Figure 1 except for monoenergetic X rays

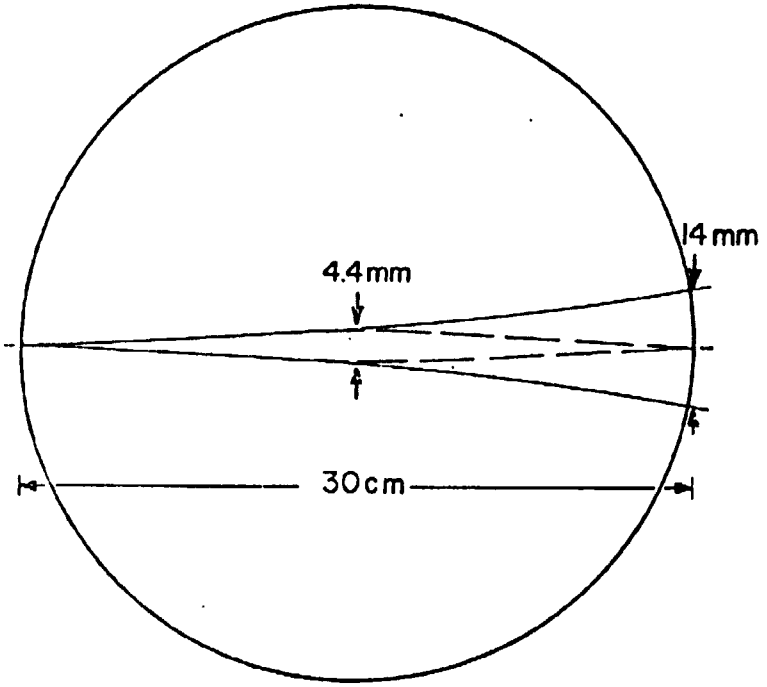

Figure 3

Proton beam spreading (FWHM) with measurement of exit position, dashed line and without, solid line.

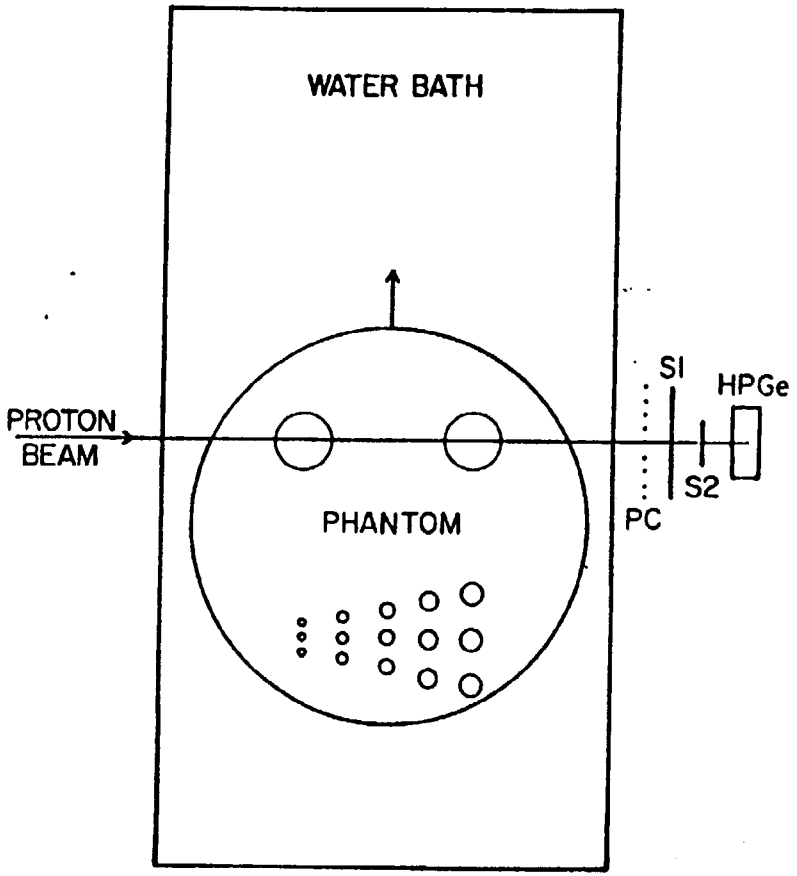

Figure 4

Experimental setup.

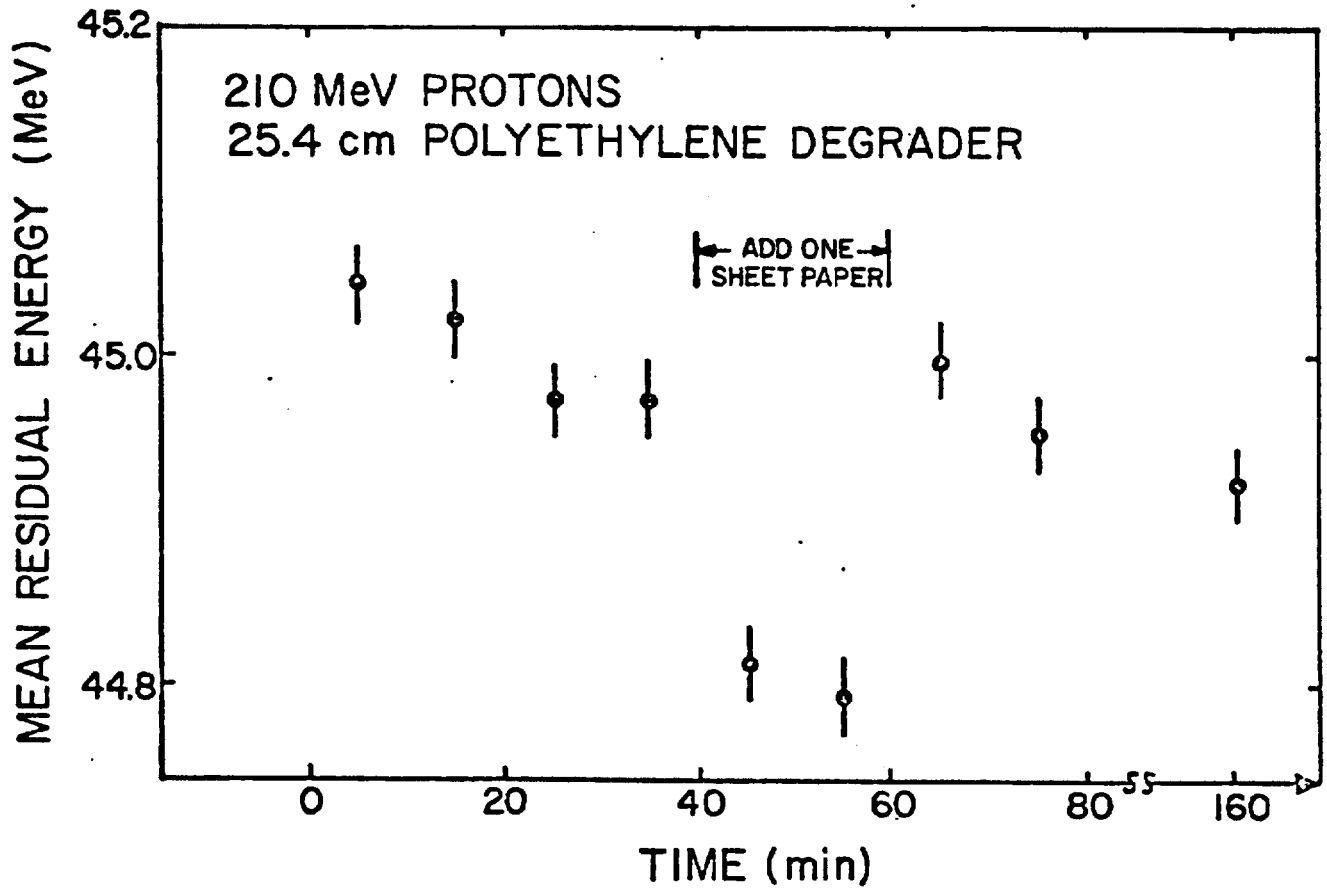

Figure 5. Measurement of the mean residual energy of a proton beam of 0.2% momentum spread, obtained in a series of nine runs, each run containing ~ 40 000 events.

V. PION BIOMEDICAL PROGRAM

A. Background

As a result of a jointly funded construction program by ERDA and NCI, a dedicated facility at LAMPF is now available for biomedical studies and clinical trials using negative pions. The facility consists of a pion beam channel, a computer and peripheral equipment for operating and monitoring the channel, data acquisition systems, and areas for research and treatment activities. The facility is operated about one-half time for a series of clinical studies to evaluate pion cancer radiotherapy (supported by the NCI) and one-half time for fundamental physical and radiobiological studies aimed at understanding and applying mixed-field radiation therapy, computerized dynamic control of charged particle beams, and visualization techniques. The DBER program supports these latter activities in terms of channel operation, beam line control systems and software development, dose monitoring services, training of operations personnel, and pion beam diagnostic measurements.

B. Biomedical Channel Development

The biomedical channel is controlled by a dedicated computer. Hardware and software developments over the past two years have provided the capability for the computerized moving of slits and wedges in the channel, setting of magnet currents, monitoring of dose rates and integrated dose, and acquisition of various kinds of data. A catalog of beam tunes and hardware settings is available which provides reasonably uniform dose distributions from stopping pions for many volumes ranging from $2 \times 2 \times 2$ cm^3 to $12 \times 12 \times 12$ cm^3. The stopping pion distribution along the beam axis is controlled by a dynamic range shifter which can easily be programmed to provide any desired physical depth dose distribution e.g., flat, uniformly sloped, curved, etc. Considerable documentation exists for many beams which generally includes the detailed three-dimensional dose distribution, distribution of low, medium and high LET components, and muon and electron contamination. The primary dose monitor is a large ionization chamber at the channel exit which is calibrated for specific experiment configurations using small ion chambers.

Facilities available include small animal holding area, animal preparation laboratory, sterile tissue culture laboratory, and a 300 keV_p x-ray machine for controlled experiments. Equipment available includes a Coulter cell counter, autoclave, incubator, freezer, and distilled water generator.

At 300 μA proton current, dose rates for several irradiation volumes (the last dimension being depth) are as follows:

$2 \times 2 \times 2$ cm^3	100 rads/min
$5 \times 5 \times 10$ cm^3	20 rads/min
$10 \times 8 \times 8$ cm^3	8 rads/min

C. Pion Research (MP-Division)

Dosimetry of negative pion beams is generally in a more primitive state than that of conventional radiations. Basic data have recently been acquired in several areas. The effects on pion dosimetry of ionization chamber size, shape, and material have been studied. The fraction of the dose from delta rays associated with pions has been determined to be 5-10% by use of an extrapolation chamber. Several investigations have been performed of the dose, RBE, and radiation quality of the neutrons (arising from room background and π^- capture) in the regions in and around the irradiation volume. Microdosimetry measurements for small and large volume pion beams have been obtained for comparison with radiobiology results.

A system has been developed to measure the number of pions per unit area by use of activation techniques. Disks of plastic scintillator are placed in the beam and irradiated for several minutes. After the irradiation, an off-line measurement is made to determine the β^+ activity from ^{11}C produced in the plastic. Cross sections for the reaction $^{12}C(\pi^-,\pi^-n)^{11}C$ were then used to determine absolute fluences. An initial check on the relative precision of this method showed it to be reproducible to $\sim \pm$ 3%. This value could be improved, if necessary.

The W-values (energy per ion pair) for pions were determined in the following manner. A parallel plate ionization chamber, 2.5-cm-diam, was sandwiched between two disks of plastic scintillator of the same diameter. The total charge produced in the gas volume of the chamber during irradiation was measured, and the total fluence through the gas was determined by the technique described in the previous paragraph. Data were obtained with the chamber filled with air, nitrogen, argon, methane-based tissue-equivalent gas, and propane-based tissue-equivalent gas; preliminary W-values for these gases for 78 ± 2 MeV π^- are 33.4 ± 2.0, 37.3 ± 1.4, 27.7 ± 1.2, 33.0 ± 2.3, and 27.0 ± 0.8 in units of eV per ion pair. These values have been corrected for the contribution from delta rays arising in the walls of the chamber.

D. Pion Research (Outside Users)

The current multidisciplinary research program with negative pi mesons at the biomedical facility includes experiments concerned with radiobiology, dosimetry and microdosimetry, visualization, pion capture, new detector systems,

and clinical trials of pion cancer radiotherapy. Approximately one-half of the beam time is allotted for research specifically designated in the NCI-sponsored program, jointly conducted by UNM and LASL (MP-Div.), to evaluate pions for cancer therapy. The remaining one-half beam time is available for other research (which, of course, may also prove relevant to the clinical program) by investigators from other institutions. To date scientists from 14 other institutions have received approval for 18 experiments, of which 11 have been completed. Institutions, experiment titles, and experiment status are listed in Appendix I. Support for the non-LASL/UNM users is provided through the DBER program. This support ranges from low-level effort in assisting with experiment setup and channel operation to full-fledged participation in the experiment.

Some of the experiments for which major phases have been completed are listed below with references.

- High LET particle detection with plastic track detectors and and nuclear emulsion (1)
- LET measurements in meson beams
- Fragments from π^- capture on C (2)
- π^- capture probabilities in tissue
- Visualization of stopping pion distributions (3)
- Normal tissue repair from π^- irradiation (4)
- Effects of π^- on mouse bone marrow cells (5), (6)
- DNA strand breaks by π^-
- Biological effects (RBE, OER) in plateau and peak (7) - (10)

REFERENCES

1. J.C. Allred, J.N. Bradbury, L. Rosen, E.V. Hungerford, H.P. Kidder, W.E. Osborne, G.C. Phillips, "Pion Radiotherapy: Studies with Nuclear Emulsions," submitted to Phys. Med. Biol.

2. J. Comiso, T. Meyer, F. Schlepuetz, and K.O. H. Ziock, "Measurement of the α-Particle Spectrum Resulting from π^- Capture in ^{12}C," Phys. Rev. Lett. 35, 13 (1975).

3. H. Daniel, J. Reidy, R. Hutson, J. Bradbury, and J. Helland, "Two-dimensional Visualizations of Stopping Pion Distribution," Rad. Res. 68, 171-176 (1976).

4. J. Fike, E. Gillette, J. Dicello, "Response of the Microvasculature to Negative Pi Mesons and Cobalt-60 Irradiation". Submitted to Radiology.

5. D.E. Carlson and J. Thornton, "Relative Biological Effectiveness of Negative Pions for the Immune Response in Mice", Radiology 118, 443 (1976).

6. D. Carlson and J. Thronton, "Effects of Negative Pi Mesons on Mouse Bone Marrow Cells", Radiology 120, 213 (1976).

7. M. Raju, H. Amols, E. Bain, S. Carpenter, J. Dicello, J. Frank, R. Tobey and R. Walters, "Biological Effects of Negative Pions". In press Int. J. of Rad. Oncology, Biology, and Physics.

8. M.R. Raju, H.I. Amols, E. Bain, S.G. Carpenter, R.A. Cox, and J.B. Robertson, "OER and RBE for Negative Pions of Different Peak Widths". Submitted to British Journal of Radiology.

9. M.R. Raju, H.I. Amols, E. Bain, S.G. Carpenter, R.A. Cox, and J.B. Robertson, "Cell Survival as a Function of Depth for Modulated Negative Pion Beams". Submitted to International Journal of Radiation Oncology, Biology, and Physics.

10. M.R. Raju, H.I. Amols, R.A. Tobey, and R.A. Walters, "Age Response for Line CHO Chinese Hamster Cells Exposed to Peak Negative Pions". Submitted to Radiation Research.